# Kinetic Modeling of Rhodium-Catalyzed Reductive Amination of Undecanal in Different Solvent Systems

**Sabine Kirschtowski[1,*], Christof Kadar[2], Andreas Seidel-Morgenstern[1,3], and Christof Hamel[1,4]**

**DOI:** 10.1002/cite.201900135



Supporting Information available online

The homogenously rhodium-catalyzed reductive amination of 1-undecanal was performed in two different thermomorphic solvent systems with the ligand Xantphos. The influences of partial pressure, temperature, methanol and catalyst concentration on the reaction were investigated. Based on a network analysis a kinetic model was derived and successfully parametrized for all studied solvent systems. Simulation results were found to be in good agreement with the experiments and allow a further process development and optimization.

**Keywords:** Homogenous catalysis, Kinetic modeling, Reductive amination, Rhodium catalysis

*Received:* September 09, 2019; *revised:* December 12, 2019; *accepted:* February 05, 2020

## 1 Introduction

Amines are a sufficient and irreplaceable basic chemical which have great importance in the production of bulk and fine chemicals such as polymers, dyes, pigments, agrochemicals, pharmaceuticals, and solvents [1–3]. Besides other processes, the reductive amination (RA) of aldehydes or ketones offers a direct and efficient way to form carbon-nitrogen bonds without toxic waste. In industrial scale the RA reaction is performed with heterogeneous catalysts, although they generally display poor chemoselectivity or toxic by-products [4–6]. As a result, more research work is being invested in providing a sustainable homogeneously catalyzed RA. As reported by Kalck et. al. [3] the addition of a primary, secondary or tertiary amine leads to a condensation of the carbonyl compound and formation of an imine/enamine-intermediate with elimination of water. In a second step the imine/enamine-intermediate is reduced to the desired amine (Fig. 1).

The RA by the so-called transfer hydrogenation enables the hydrogenation without adding hydrogen gas, however specially designed, costly and often non-recyclable homogeneous transition metal catalysts (Ru, Ir) and hydrogen donor molecules are needed [7–12]. For a sustainable and economic catalytic process, the reuse of the catalyst plays a key role, so to enable the reusability of the catalysts, Au or Rh nanoparticles [3, 13] or homogeneous catalysts based on Rh, Ir, and Ru complexes [14–19] can be used. Moreover, to increase the effectiveness of the RA reaction pure hydrogen gas should be applied and solved in an innovative solvent system, respectively.

One versatile and elegant strategy for the recovery and the recycling of homogeneous transition metal catalysts is the application of thermomorphic multiphase systems (TMS). As reported by [20], the TMS will be applied to a wide variety of reactions as they allow both, a homogeneous reaction at reaction temperature and a common liquid-liquid separation at room temperature. This can be achieved by two solvents of different polarity, which have a temperature-controlled miscibility gap [20, 21].

In terms of process development, control and optimization, knowledge about the reaction kinetics is of crucial importance. In this contribution, reaction kinetics of the

[1]Sabine Kirschtowski, Prof. Andreas Seidel-Morgenstern, Prof. Christof Hamel
sabine.kirschtowski@ovgu.de
Otto von Guericke University Magdeburg, Institute of Process Engineering, Universitätsplatz 2, 39106 Magdeburg, Germany.

[2]Christof Kadar
Nuremberg Institute of Technology, Faculty of Applied Chemistry, Keßlerplatz 12, 90489 Nuremberg, Germany.

[3]Prof. Andreas Seidel-Morgenstern
Max Planck Institute for Dynamic of Complex Technical Systems, Sandtorstrasse 1, 39106 Magdeburg, Germany.

[4]Prof. Christof Hamel
Anhalt University of Applied Sciences, Process Engineering, Bernburger Strasse 55, 06354 Köthen, Germany.

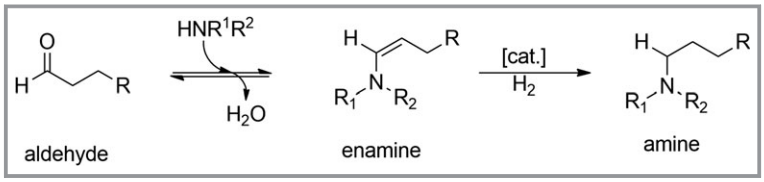


**Figure 1.** Exemplary reaction equation of a reductive amination of an aldehyde with a secondary amine [2].

Rh/Xantphos-catalyzed reductive amination of 1-undecanal in a TMS consisting of MeOH/dodecane with different compositions is being experimentally and model-based investigated.

## 2 Experimental

Reductive amination experiments were conducted in a high-pressure, stainless-steel batch Parr reactor equipped with a glass stirrer, a gas supply system, a pressure regulator and a temperature controller [22, 23]. For the standard experiments the composition of MeOH/dodecane = 99:1 wt %/wt % was chosen. The catalyst solution was prepared by dissolving Rh(acac)COD (0.009 mmol) and Xantphos (0.018 mmol) in the solvent methanol (1151 mmol, 99.8 %). Subsequently, the reactor was filled with diethylamine (9.060 mmol, 99.5 %) and dodecane (2.186 mmol, 99 %). The solution was heated to the reaction temperature and the catalyst preparation was initialized after pressurizing with $H_2$ (99.9 %). The kinetic experiment began with the controlled injection of 1-undecanal (Sub, 9.060 mmol, 97 %), thus, the starting input were Rh/P/Sub = 1:2:1000 mol/mol/mol and DEA/Sub = 1:1 mol/mol. Liquid samples were taken and analyzed with standard gas chromatography. Each run was repeated at least twice to ensure reproducibility of the results. The reproducibility of the kinetic experiments in terms of the variation coefficient of the desired amine after 120 min was always < 3 %. Details to the experimental procedure and the quantitative analysis can be found in the Supporting Information (SI).

### 2.1 Reaction Network and Experimental Results

In preliminary investigations, four reaction products of the reductive amination were identified. In addition to the expected enamine intermediate and the desired amine, alcohols and aldols could be detected as minor by-products. Thus, a more precise reaction network could be postulated (Fig. 2). Alcohols were formed by the catalytic hydrogenation of the substrate 1-undecanal, whereas the aldols are formed by the organocatalyzed aldol reaction. Because of the wide variety of aldol products, they were categorized as a pseudo-component, namely aldols.

For the kinetic description of the reductive amination the influences of the temperature $T$ and the partial pressure $p_{H2}$ was investigated ranging from 85–115 °C and 10–30 bar, respectively. In addition, the influence of the diethylamine content $\alpha_{D:U}$ and the catalyst concentration related to the substrate $x_{cat}$ was examined. In order to increase the sensitivity of the parameter for the following estimation, perturbation experiments with high information content were performed. The process parameters $T$ and $p_{H2}$ were changed during these experiments dynamically. Overall more than 24 experiments were done and the yields of the amine $Y_{amine}$ were summarized in Tab. 1. The solvent composition of MeOH/Dod was changed between 50:50 and 99:01.

Tab. 1 reveals the influence of the methanol content is negligible, so that the experiments with the TML consisting of MeOH/Dod = 50:50 are comparable to the experiments in the homogeneous system. By increasing the amount of the DEA in the homogeneous system, a significant increase in the amine yield $Y_{amine}$ can be achieved. Moreover, the reduction of the catalyst concentration did not lead to significant changes in the amine yields in the parameter range considered. Only by changing temperature and pressure dynamically during the experiments, an increase in the amine yield could be achieved (Tab. 1, Exp. 7).

## 3 Kinetic Description

A literature study revealed, there is no reliable reaction kinetics for the homogenous catalyzed RA available. For a first kinetic model a simplified description of the reaction network was used. In that the aldehyde/enamine equilibri-

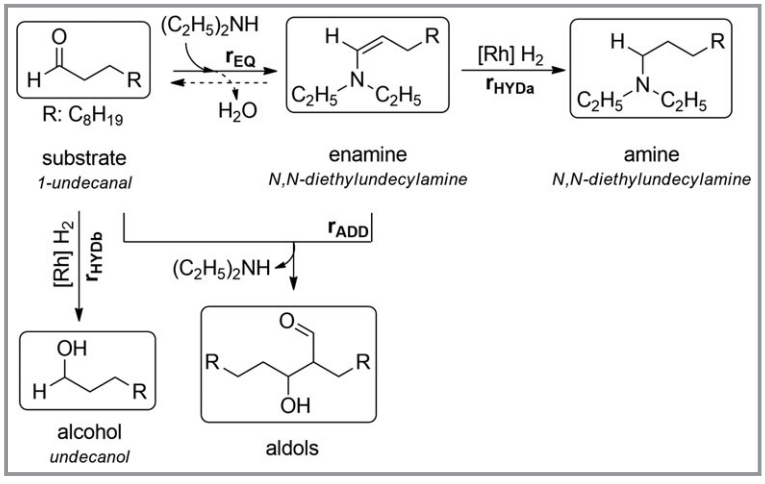


**Figure 2.** Proposed reaction network of the reductive amination of 1-undecanal.

  

**Table 1.** Experimental results for the reductive amination of 1-undecanal after 120 min.

| Experiment | 1[a)] | 2 | 3 | 4 | 5[a),b)] | 6[a),b)] | 7[a),b)] |
|---|---|---|---|---|---|---|---|
| MeOH/Dod | 99:01 | 99:01 | 99:01 | 99:01 | 99:01, | 99:01 | 99:01 |
| | 50:50 | | | | 50:50 | 50:50 | 50:50 |
| $\alpha_{D:U}$ [–] | 1 | 4 | 1 | 1 | 1 | 1 | 1 |
| $x_{cat}$ [mol %] | 0.1 | 0.1 | 0.05 | 0.025 | 0.1 | 0.1 | 0.1 |
| $P_{H2}$ [bar] | 20 | 20 | 20 | 20 | 10-30 | 20 | 10-30 |
| $\theta$ [°C] | 100 | 100 | 100 | 100 | 100 | 85-115 | 85-115 |
| $Y_{amine}$ [%] | 92.3 ± 1.3 | 95.8 ± 0.5[c)] | 86.5 ± 5.6 | 88.8 ± 1.2 | 93.5 ± 0.2 | 93.3 ± 1.2 | 95.6 ± 0.1 |
| | 92.4 ± 1.1 | | | | 95.5 ± 1.0 | 91.3 ± 1.9 | 95.4 ± 1.2 |

Fixed reaction conditions: $\alpha_{Rh:P}$ = 1:2, $w_{sub}$ = 4 wt %. a) In each case individual experiments were carried out for the respective solvent systems. b) Perturbation experiment (temperature/pressure profiles in Fig. 4 and the SI). c) Maximum yield reached after $t$ = 20 min.

um is shifted completely to the product side. The elimination of water is neglected due to the small amount of < 1 % (Fig. 2, dotted lines) measured during the experiments. The material balance of a well-mixed batch reactor was applied for each component $i$ (Eq. (1)) in the liquid phase.

$$\frac{dc_i}{dt} = \beta_{eff}\left(c_{H_2}{}^{\star} - c_{H_2}\right) + \sum_{j=1}^{M} \nu_{ij} r_j \tag{1}$$

Henry's law (Eq. (3)) was used to describe the gas solubility of $H_2$ to the liquid phase. In preliminary gas solubility experiments the Henry coefficient $H_{H2}$ and the mass transfer coefficient $\beta_{eff}$ could be determined. Details to the experimental procedure can be found in the SI. A significant temperature dependence of the Henry coefficient in the investigated temperature range could not be determined, so mean values were used in the parameter range studied (Tab. 2).

**Table 2.** Gas solubility and mass transfer parameters for $H_2$ in the TMS MeOH/Dod.

| MeOH/Dod | 99:1 [%] | 50:50 [%] |
|---|---|---|
| $H_{H2}$ [bar Lmol$^{-1}$] | 239 ± 2.6 | 298 ± 5 |
| $\beta_{eff}$ [s$^{-1}$] | 0.0309 ± 3.0 | 0.0365 ± 9.4 |

$$\frac{dp_i}{dt} = \beta_{eff}\left(p_i{}^{\star} - p_i\right) \tag{2}$$

$$c_{H_2}{}^{\star} = \frac{p_{H_2}}{H_{H_2}} \tag{3}$$

To describe the experimental results a power-law approach was applied for the hydrogenations $r_{HYDa}$ and $r_{HYDb}$ as well as the condensation $r_{EQ}$ and the organocatalytic addition $r_{ADD}$ (Eqs. (4)–(7)).

$$r_{EQ} = k_{EQ}(T) c_{Sub}^{\gamma_{EQ}} c_{DEA}^{\delta_{EQ}} \tag{4}$$

$$r_{HYDa} = k_{HYDa}(T) c_{cat} c_{En}^{\gamma_{HYDa}} c_{H_2}^{\delta_{HYDa}} \tag{5}$$

$$r_{HYDb} = k_{HYDb}(T) c_{cat} c_{Sub}^{\gamma_{HYDb}} c_{H_2}^{\delta HYDb} \tag{6}$$

$$r_{ADD} = k_{ADD}(T) c_{Sub}^{\gamma_{ADD}} c_{En}^{\delta_{ADD}} \tag{7}$$

The dependence of the reaction rate constant $k$ on the temperature was determined by Arrhenius (Eq. 8).

$$k_j = k_{0,j} \exp\left(\frac{E_{A,j}}{RT}\right) \tag{8}$$

## 4 Parameter Estimation and Simulation

By adapting four reaction pathways with four free parameters (italic) each (Eq. (9)), the complexity of the model increases significantly. For this reason, the free parameters were reduced by supposing the reaction orders as one (Eq. (10)). This assumption is in good agreement with existing hydrogenation models for imines [24–27] and mechanistic model approaches [28].

The parameters in Eq. (10) were estimated with using the lsqnonlin solver. Based on the nonlinear least-square algorithm the absolute difference of model and experimental values was minimized by the objective function (OF) (Eq. (11)).

$$\bar{\Theta} = \begin{bmatrix} k_{0,EQ}, & k_{0,HYDa}, & k_{0,HYDb}, & k_{0,EQ}, \\ E_{A,EQ}, & E_{A,HYDa}, & E_{A,HYDb}, & E_{A,ADD}, \\ \gamma_{EQ}, & \gamma_{HYDa} & \gamma_{HYDb}, & \gamma_{ADD}, \\ \delta_{EQ}, & \delta_{HYDa}, & \delta_{HYDb}, & \delta_{ADD} \end{bmatrix} \tag{9}$$

$$\bar{\Theta}^{red} = \begin{bmatrix} k_{0,EQ}, & k_{0,HYDa}, & k_{0,HYDb}, & k_{0,ADD}, \\ E_{A,EQ}, & E_{A,HYDa}, & E_{A,HYDb}, & E_{A,ADD} \end{bmatrix} \tag{10}$$

$$OF = \min_{\bar{\theta}^{red}} RSS = \sum_{i=1}^{N} \sum_{n=1}^{N_{exp}} \sum_{m=1}^{N_{sp}} \left[ \left| c_{i,n}^{mod}\left(t_m, \bar{\theta}\right) - c_{i,n}^{exp}(t_m) \right| \right]^2 \tag{11}$$

In Figs. 3 and 4 selected simulation results are summarized. More information and the related parity plots can be found in the SI. It can be recognized, that a reduced kinetic model and the experimental profiles are in good agreement. The finally used parameters and their 95 % confidence intervals (CI) are given in Tab. 3.

  

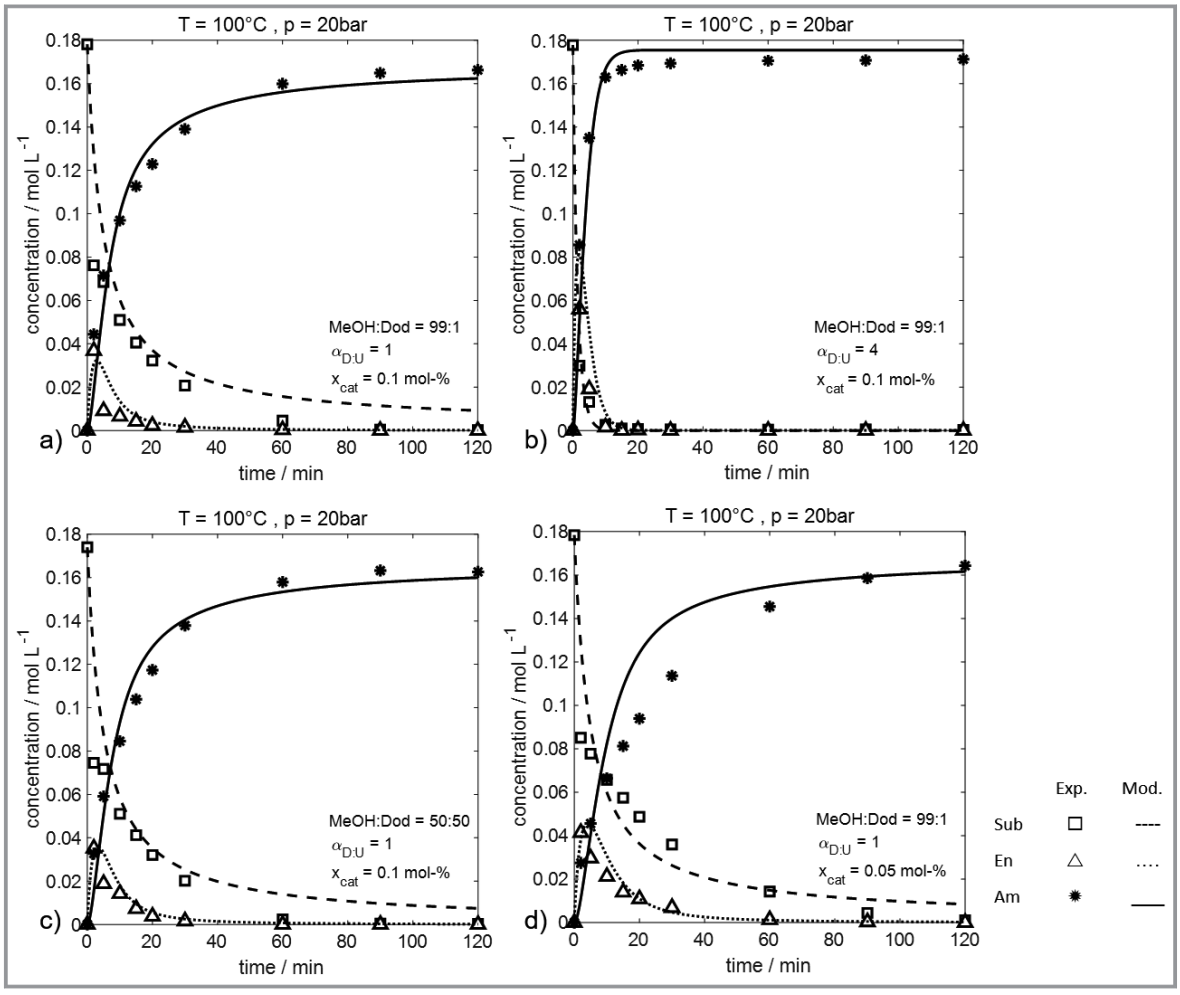


**Figure 3.** Experimental (symbols) and simulation results (lines) for two different solvent systems: undecanal (□,–), enamine (△,…) and amine (★, __). Subfigure a and c are related to table 1/exp. 1, subfigure b to table1/exp. 2 and subfigure d to table 1/exp. 3. For reasons of clarity results for the alcohol and the aldols are not shown.

**Table 3.** Estimated Parameters.

| | Parameter | Estimated values |
|---|---|---|
| EQ | $k_{0,EQ}$ [L mol$^{-1}$min$^{-1}$] | 39.608 |
| | $E_{A,EQ}$ [kJ mol$^{-1}$] | 10.911 |
| HYDa | $k_{0,HYDa}$ [L mol$^{-1}$min$^{-1}$] | $2.528 \cdot 10^7$ |
| | $E_{A,HYDa}$ [kJ mol$^{-1}$] | 20.344 |
| HYDb | $k_{0,HYDb}$ [L mol$^{-1}$min$^{-1}$] | $2.249 \cdot 10^8$ |
| | $E_{A,HYDb}$ [kJ mol$^{-1}$] | 46.696 |
| ADD | $k_{0,ADD}$ [L mol$^{-1}$min$^{-1}$] | 612.483 |
| | $E_{A,ADD}$ [kJ mol$^{-1}$] | 28.123 |

All confidence intervals < 1 %.

All parameters in Tab. 3 have small confidence intervals, emphasizing the statistical significance of the estimated parameters. Although less $H_2$ dissolves in the liquid phase due to the lower MeOH content in the TML MeOH/Dod = 50:50 (Tab. 2), the $H_2$ content in the solvent is not a limiting factor (Fig. 3a)/b)/d)). Thus, the model is able to reproduce both the TML MeOH/Dod = 50:50 (Fig. 3c)) and the homogeneous solvent MeOH/Dod = 99:01 (Fig. 3a)). The perturbation experiment in the TMS could be described better in comparison to the homogeneous solvent (Fig. 4). Due to the temperature-independent Henry-coefficient the maximum yield of the amine is not exactly match by the simulation. Nevertheless, the estimated parameters and the model were also able to describe dynamic experiments by perturbations very well. The deviation between model and experiment at the enamine intermediate are due limitations in the analytics.

The activation energy for the hydrogenation of the enamine to the desired amine was estimated to be around 20 kJ mol$^{-1}$. A quite similar value about 22.59 kJ mol$^{-1}$ was found by Landaeta [18] for the hydration of *N*-(β-naphthylmethylene)aniline (NβNA) in THF with a Rh catalyst in a temperature range from 31–50 °C.

  

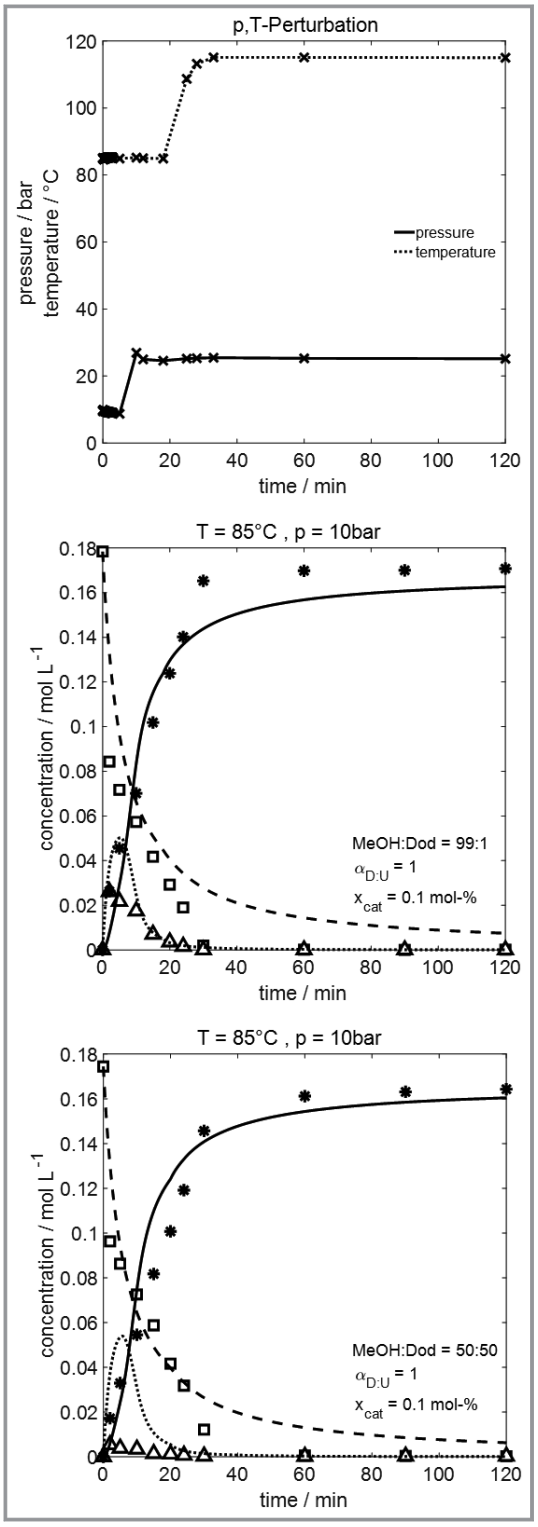


**Figure 4.** Perturbation experiments for two different TMS: Experimental (symbols) and simulation results (lines) for undecanal (□,–), enamine (△,…) and amine (★, __). The results related to table 1/exp. 7. For reasons of clarity results for the alcohol and the aldols are not shown.

## 5 Discussion

The Rh/Xantphos homogeneously catalyzed reductive amination of 1-undecanal was investigated in two different temperature-controlled solvent systems, a temperature and a pressure range from 85–115 °C and 10–30 bar, respectively. Moreover, the influences of the diethylamine content and the catalyst concentration were studied. A successful kinetic adaptation to the experimental data was achieved by a reduced kinetic approach. Both, the main reaction pathway and the minor by-products could be described well in static and dynamic experiments based on the kinetic model.

For a more detailed description with regard to continuous reaction processes including recycle streams, the aldehyde/enamine equilibrium must be considered in the kinetic estimation. In particular, the influence of the formed and accumulated water cannot be neglected, since it influences both, hydrogen solubility and equilibrium. By consideration of the equilibrium, similar to the *n*-alkene/*iso*-alkene equilibrium in the hydroformylation [29], in the mathematical description, the reversibility of the aldehyde-enamine equilibrium may be described. The experimental analysis and developed model provide a good basis to perform a first feasibility study and process design of a promising homogenous way of the RA.

## Supporting Information

Supporting Information for this article can be found under DOI: https://doi.org/10.1002/cite.201900135. This section includes additional references to primary literature relevant for this research [30, 31].

Gefördert durch die Deutsche Forschungsgemeinschaft (DFG) – TRR 63 "Integrierte chemische Prozesse in flüssigen Mehrphasensystemen" (Teilprojekt X1) – 56091768. This work is embedded into the collaborative research center SFB/TR 63 – Integrated Chemical Processes in Liquid Multiphase Systems – InPROMPT and the authors would like to thank the German Science Foundation (DFG) for the financial support. We are also very grateful to Umicore Ag and Co. KG for the supply of the catalyst precursor.

## Symbols used

| | | |
|---|---|---|
| $k_{0,j}$ | $[L^n mol^{-n} min^{-1}]$ | collision factor of reaction *j* |
| $c$ | $[mol\ L^{-1}]$ | concentration |
| $E_A$ | $[J\ mol^{-1}]$ | activation energy |
| $H$ | $[bar\ L\ mol^{-1}]$ | Henry coefficient |
| $j$ | $[mol\ L^{-1} min^{-1}]$ | flux |
| $j_{H2}$ | $[bar\ min^{-1}]$ | flux of hydrogen partial pressure |

  

| | | |
|---|---|---|
| $k$ | [L mol$^{-1}$min$^{-1}$] | reaction rate constant |
| $M$ | [–] | number of reactions |
| $N$ | [–] | number of components |
| $N_{exp}$ | [–] | number of experiments |
| $N_{sp}$ | [–] | number of sample points |
| $p$ | [bar] | pressure |
| $r$ | [mol L$^{-1}$min$^{-1}$] | reaction rate |
| $T$ | [K] | temperature |
| $t$ | [min] | time |
| $w$ | [wt %] | substrate concentration |
| $x$ | [mol %] | catalyst concentration |
| $Y_{amine}$ | [%] | yield of the amine |

## Greek symbols

| | | |
|---|---|---|
| $\alpha$ | [mol mol$^{-1}$] | molar ratio |
| $\beta_{eff}$ | [s$^{-1}$] | effective mass transfer |
| $\gamma$,$\delta$ | [–] | reaction order |
| $\Theta$ | [–] | parameter vector |
| $\theta$ | [°C] | temperature |
| $\nu$ | [–] | stoichiometric coefficient |

## Sub- and Superscripts

| | |
|---|---|
| * | equilibrium |
| ADD | addition |
| cat | catalyst |
| EQ | equilibrium |
| exp | experiment |
| HYDa | hydrogenation a |
| HYDb | hydrogenation b |
| i | component indicator |
| j | reaction indicator |
| m | sample point indicator |
| mod | model |
| n | number of experiment indicator |
| red | reduced |

## Abbreviations

| | |
|---|---|
| DEA | diethylamine |
| Dod | dodecane |
| En | enamine |
| MeOH | methanol |
| NMPA | naphthalene-2-ylmethylpjhenylamine |
| NβNA | *N*-(β-naphthylmethylene)aniline |
| OF | objective function |
| RA | reductive amination |
| RSS | residual sum of square |
| Sub | substrate |
| THF | tetrahydrofuran |

## References


[1] R. S. Downing, P. J. Kunkeler, H. van Bekkum, *Catal. Today* **1997**, *37 (2)*, 121–136. DOI: https://doi.org/10.1016/S0920-5861(97)00005-9

[2] P. Eilbracht, L. Bärfacker, C. Buss, C. Hollmann, B. E. Kitsos-Rzychon, C. L. Kranemann, T. Rische, R. Roggenbuck, A. Schmidt, *Chem. Rev.* **1999**, *99 (11)*, 3329–3366. DOI: https://doi.org/10.1021/cr970413r

[3] P. Kalck, M. Urrutigoity, *Chem. Rev.* **2018**, *118*, 3833–3861. DOI: https://doi.org/10.1021/acs.chemrev.7b00667

[4] K. S. Hayes, *Appl. Catal. A* **2001**, *221 (1–2)*, 187–195. DOI: https://doi.org/10.1016/S0926-860X(01)00813-4

[5] S. Gomez, J. A. Peters, T. Maschmeyer, *Adv. Synth. Catal.* **2002**, *344 (10)*, 1037–1057. DOI: https://doi.org/10.1002/1615-4169(200212)344:10<1037:AID-ADSC1037>3.0.CO;2-3

[6] A. W. Heinen, J. A. Peters, H. v. Bekkum, *Eur. J. Org. Chem.* **2000**, *2000 (13)*, 2501–2506. DOI: https://doi.org/10.1002/1099-0690(200007)2000:13<2501::AID-EJOC2501>3.0.CO;2-S

[7] O. S. Nayal, V. Bhatt, S. Sharma, N. Kumar, *J. Org. Chem.* **2015**, *80 (11)*, 5912–5918. DOI: https://doi.org/10.1021/acs.joc.5b00156

[8] Q. Lei, Y. Wei, D. Talwar, C. Wang, D. Xue, J. Xiao, *Chemistry* **2013**, *19 (12)*, 4021–4029. DOI: https://doi.org/10.1002/chem.201204194

[9] C. Wang, A. Pettman, J. Basca, J. Xiao, *Ang. Chem. Int. Ed.* **2010**, *49 (41)*, 7548–7552. DOI: https://doi.org/10.1002/anie.201002944

[10] D. Gülcemal, S. Gülcemal, C. M. Robertson, J. Xiao, *Organometallics* **2015**, *34 (17)*, 4394–4400. DOI: https://doi.org/10.1021/acs.organomet.5b00625

[11] L. Jiang, P. Zhou, Z. Zhang, S. Jin, Q. Chi, *Ind. Eng. Chem. Res.* **2017**, *56 (44)*, 12556–12565. DOI: https://doi.org/10.1021/acs.iecr.7b03621

[12] D. Talwar, N. P. Salguero, C. M. Robertson, J. Xiao, *Chemistry* **2014**, *20 (1)*, 245–252. DOI: https://doi.org/10.1002/chem.201303541

[13] S. Liang, P. Monsen, G. B. Hammond, B. Xu, *Org. Chem. Front.* **2016**, *3 (4)*, 505–509. DOI: https://doi.org/10.1039/c5qo00439j

[14] T. Gross, A. M. Seayad, M. Ahmad, M. Beller, *Org. Lett.* **2002**, *4 (12)*, 2055–2058. DOI: https://doi.org/10.1021/ol0200605

[15] V. I. Tararov, R. Kadyrow, T. H. Riermeier, A. Börner, *Chem. Comm.* **2000**, *2000 (19)*, 1867–1868. DOI: https://doi.org/10.1039/b005777k

[16] Vitali Tararov, Renat Kadyrov, Thomas Riermeier, Karl-Josef Haack, Uwe Dingerdissen, Armin Boerner, *US Patent 6 884 887 B1*, **2005**.

[17] T. Senthamarai, K. Murugesan, J. Schneidewind, N. V. Kalevaru, W. Baumann, H. Neumann, P. C. J. Kamer, M. Beller, R. V. Jagadeesh, *Nat. Commun.* **2018**, *9*, 4123. DOI: https://doi.org/10.1038/s41467-018-06416-6

[18] J. Gallardo-Donaire, M. Hermsen, J. Wysocki, M. Ernst, F. Rominger, O. Trapp, A. S. K. Hashmi, A. Schäfer, P. Comba, T. Schaub, *J Am. Chem. Soc.* **2018**, *140 (1)*, 355–361. DOI: https://doi.org/10.1021/jacs.7b10496

[19] J. Gallardo-Donaire, M. Ernst, O. Trapp, T. Schaub, *Adv. Synth. Catal.* **2016**, *358 (3)*, 358–363. DOI: https://doi.org/10.1002/adsc.201500968

[20] J. Bianga, K. U. Künnemann, T. Gaide, A. J. Vorholt, T. Seidensticker, J. M. Dreimann, D. Vogt, *Chem. Eur. J.* **2019**, *25 (50)*, 11586–11608. DOI: https://doi.org/10.1002/chem.201902154

[21] J. M. Dreimann, T. A. Faßbach, S. Fuchs, M. R. L. Fürst, T. Gaide, R. Kuhlmann, K. A. Ostrowski, A. Stadler, T. Seidensticker, D. Vogelsang, H. W. F. Warmeling, A. J. Vorholt, *Chem. Ing. Tech.* **2017**, *89 (3)*, 252–262. DOI: https://doi.org/10.1002/cite.201600119


  

[22] G. Kiedorf, D. M. Hoang, A. Müller, A. Jörke, J. Markert, H. Arellano-Garcia, A. Seidel-Morgenstern, C. Hamel, *Chem. Eng. Sci.* **2014**, *115*, 31–48. DOI: https://doi.org/10.1016/j.ces.2013.06.027
[23] M. Gerlach, S. Kirschtowski, A. Seidel-Morgenstern, C. Hamel, *Chem. Ing. Tech.* **2018**, *90 (5)*, 673–678. DOI: https://doi.org/10.1002/cite.201700162
[24] C. A. Willoughby, S. L. Buchwald, *J. Am. Chem. Soc.* **1994**, *116 (26)*, 11703–11714. DOI: https://doi.org/10.1021/ja00105a011
[25] V. R. Landaeta, B. K. Muñoz, M. Peruzzini, V. Herrera, C. Bianchini, R. A. Sánchez-Delgado, *Organometallics* **2006**, *25 (2)*, 403–409. DOI: https://doi.org/10.1021/om0504912
[26] V. Herrera, B. Muñoz, V. Landaeta, N. Canudas, *J. Mol. Catal. A* **2001**, *174 (1–2)*, 141–149. DOI: https://doi.org/10.1016/S1381-1169(01)00197-2
[27] C. R. Landis, J. Halpern, *J. Am. Chem. Soc.* **1987**, *109 (6)*, 1746–1754. DOI: https://doi.org/10.1021/ja00240a025
[28] *Kinetics of Multistep Reactions*, 2nd ed. (Ed: F. G. Helfferich), Elsevier, Amsterdam **2004**.
[29] A. Jörke, A. Seidel-Morgenstern, C. Hamel, *Chem. Eng. J.* **2015**, *260*, 513–523. DOI: https://doi.org/10.1016/j.cej.2014.09.015
[30] R. Sander, *Atmos. Chem. Phys.* **2015**, *15 (8)*, 4399–4981. DOI: https://doi.org/10.5194/acp-15-4399-2015
[31] M. Schwaab, J. C. Pinto, *Chem. Eng. Sci.* **2007**, *62 (10)*, 2750–2764. DOI: https://doi.org/10.1016/j.ces.2007.02.020

  